Video Article

Artificial Thermal Ageing of Polyester Reinforced and Polyvinyl Chloride Coated Technical Fabric

Paweł Kłosowski[1], Krzysztof Zerdzicki[1], Krzysztof Woznica[2]

[1]Faculty of Civil and Environmental Engineering, Gdansk University of Technology

[2]Laboratoire de Mecanique Gabriel Lame, Institut National des Sciences Appliquees Centre Val de Loire

Correspondence to: Paweł Kłosowski at klosow@pg.edu.pl

Abstract

Architectural fabric AF9032 has been subjected to artificial thermal ageing to determine changes of the material parameters of the fabric. The proposed method is based on the accelerated ageing approach proposed by Arrhenius. 300 mm x 50 mm samples were cut in the warp and fill directions and placed in a thermal chamber at 80 °C for up to 12 weeks or at 90 °C for up to 6 weeks. Then after one week of conditioning at ambient temperature, the samples were uniaxially tensioned at a constant strain rate. Experimentally, the parameters were determined for the non-linear elastic (linear piecewise) and viscoplastic (Bodner–Partom) models. Changes in these parameters were studied with respect to the ageing temperature and ageing period. In both cases, the linear approximation function was successfully applied using the simplified methodology of Arrhenius. A correlation was obtained for the fill direction between experimental results and the results from the Arrhenius approach. For the warp direction, the extrapolation results exhibited some differences. Increasing and decreasing tendencies have been observed at both temperatures. The Arrhenius law was confirmed by the experimental results only for the fill direction. The proposed method makes it possible to predict real fabric behavior during long term exploitation, which is a critical issue in the design process.

Video Link

The video component of this article can be found at https://www.jove.com/video/60737/

Introduction

Polyester based architectural fabrics are commonly used for construction of hanging roofs[1]. Being relatively cheap with good mechanical properties, they can be employed in long-term exploitation (e.g., the hanging roof of the Forest Opera in Sopot - Poland). Unfortunately, weather conditions, ultraviolet radiation, biological reasons, and operational purposes (season pre-stressing and loosening[2]) can affect their mechanical properties. Hanging roofs made of AF9032 are typically seasonal structures subjected to high temperature (especially during sunny days in the summer), regular pre-tensioning and loosening. In order to properly design a hanging roof, fabric parameters must be determined not only at the beginning of exploitation, but also after several years of use.

Ageing analysis measures the ageing indicator and compares the initial and final values of the parameters to assess the impact of ageing. Cash et al.[3] proposed one of the simplest methods by comparative analysis of 12 different types of roofing membranes. These membranes were exposed to outdoor weathering for 2 or 4 years. The authors used a rating system of several properties to assess fabric durability. In order to provide an analysis of polymer thermal ageing, the time-temperature superposition principle (TTSP) can be applied[4]. This principle states that the behavior of a material at low temperature and under low strain level resembles its behavior at high temperature and high strain level. The simple multiplicative factor can be used to relate the current temperature properties with the properties at the reference temperature. Graphically, it corresponds to the curve shift on the log time scale. Regarding the temperature, two methods are proposed to combine the shift factor and the ageing temperature: the Williams-Landel-Ferry (WLF) equations, and the Arrhenius law. Both methods are included in the Swedish standard ISO 11346[5] to estimate the lifetime and maximum operational temperature for rubber, or vulcanized and thermoplastic, materials. Recently, thermal ageing and Arrhenius methodology have been used in the cable lifetime prediction[6,7], heating pipes[8], and polymer glue PMMA[4]. An extension of the Arrhenius law is the Eyring law that takes into account other ageing factors (e.g., voltage, pressure, etc.)[9]. Alternatively, other studies propose and verify simple linear models for a description of ageing (e.g., biosensor ageing[10]). Although the Arrhenius method is commonly used, there is discussion on its relevance in the lifetime prediction of every material. Hence, the method must be used with care, especially in terms of initial assumptions and experimental conditions[6].

Similar to most polymers, the polyester fabrics used in the current research exhibit two distinct transition phases defined by the melting temperature (T_m) and the glass transition temperature (T_g). The melting temperature (T_m) is the temperature when a material changes from its solid state to the liquid one, and the glass transition temperature (T_g) is the boundary between the glass and rubber states[11]. According to manufacturer's data, the AF9032 fabric is made from polyester threads (T_g = 100−180 °C[12], T_m = 250−290 °C[13]) and PVC coating (T_g = 80−87 °C[14,15], T_m = 160−260 °C[16]). The ageing temperature T_a should be selected below T_g. During sunny days, the temperature on the top surface

of a hanging roof may even reach 90 °C; thus, two ageing temperatures (80 °C and 90 °C) are tested here. These temperatures are below the thread T_g and close to the coating T_g.

The performance of the accelerated ageing protocol on technical fabrics is presented in the current work. Artificial thermal ageing is used to predict changes of the material properties. The article illustrates appropriate laboratory testing routines and a way to extrapolate relatively short-term experimental results.

Protocol

1. Accelerated thermal ageing experiments on technical fabric

1. Overall preparation
   1. Prepare a testing machine with proper software (in order to provide constant strain rate tests) and a video extensometer.
   2. Prepare a thermal chamber providing constant temperature of 80 °C (± 1 °C) and 90 °C (±1 °C) for at least 12 weeks.

2. Specimen preparation
   1. Unroll the technical fabric AF9032 bale. Draw the desired shapes (300 mm x 50 mm) with a soft pencil or marker on the fabric surface parallel to the warp or fill direction.
   NOTE: The distribution of specimens on the fabric surface is given elsewhere[17].
   2. Indicate the warp direction on each specimen with a permanent marker. Cut the specimens with a sharp knife or scissors. Use the ruler if a knife is used for cutting.
   NOTE: The specimens should be rectangular[17]. The major load-caring elements of the fabric are threads. In the operational phase, the coating material usually exceeds its yield limit, thus not taking part in the stress distribution. The only elements to carry the load are threads spreading from one grip to another. Therefore, it is not reasonable to use sophisticated shapes of specimens (e.g., a dumbbell shape usually used for metals). On the other hand, such sample shapes result in the need for special grips when the ultimate load is investigated, or the use of an extensometer in order to assess material parameters.
   3. Measure the specimen's thickness with a slide caliper and count the number of threads at the short edge of the specimen.
   NOTE: For each specimen, take three thickness measurements, and compute the average value. Use the magnifying glass to assess the number of threads if necessary.

3. Turn on the thermal chamber, leaving the door open. Using the buttons and the control display, select the temperature (80 °C). Close the thermal chamber door and observe the increase of temperature on the control panel.

4. Specimen warming
   1. When the temperature is close to 80 °C, open the thermal chamber door. Insert at least 7 sets of specimens with each set consisting of 6 specimens cut in the warp direction and 6 in the fill direction. Close the door as soon as possible in order to avoid a temperature drop.
   NOTE: The experiments should be conducted for three strain rates. For each strain rate, experiments are performed on two specimens in the warp direction and two in the fill direction. Place excess specimens in the chamber in case the experiments are not successful or the results from both tests are highly divergent.
   2. After 1 h, don thermal gloves and remove the first set of specimens (the reference set; 6 specimens in the warp direction and 6 in the fill direction). After every 2 weeks, remove a succeeding set of specimens from the thermal chamber.
   NOTE: The entire warming process will take 12 weeks.

5. Specimen conditioning
   1. Leave the specimens at room temperature for one week. Cool the specimens to room temperature (i.e., their properties should be stabilized).
   2. Before the test, draw two black marks (dots) using a permanent marker with a lengthwise separation of about 50 mm (L0) in the middle of each specimen.
   NOTE: The dots will be used by the video extensometer.

6. Testing machine setup
   1. Install four 60 mm flat inserts into the testing machine, two inserts per one grip. The inserts show a fish scale surface type and are used to avoid slipping the specimens out of the grips.
   2. Switch on the machine. Start the software (e.g., TestXpert) that controls the machine. Choose the program dedicated to the tensile tests.
   3. Select the starting position with a 200 mm grip to grip separation in the software. Click the **Starting Position** button to execute the 200 mm grip to grip separation. This grip position is usually called the starting position for a test.
   NOTE: The 200 mm distance is required by the ISO standard[17].

7. Video extensometer setup
   1. Move the camera of the video extensometer along the supporting bar to situate the lens of the camera at the level of the middle part of the specimen. Check whether the lens of the camera provides a clear view of the specimen markers during the whole experiment.
   NOTE: Perform a similar test before the main test to establish the probable sample elongation range to ensure that the camera will follow the black markers during an entire test.
   2. Select the proper brightness and focus for the lens using the computer screen and the associated software.

8. Video extensometer calibration
   NOTE: The calibration device is the standard equipment of the video extensometer.
   1. Put the calibration device in the front of the camera and clamp it with the grips.

2. Using the video extensometer software (e.g., VideoXtens), select the proper type of markers in the **Targets** window (usually black and white).
3. Select the calibration procedure in the video extensometer software using the **Scale** option and choose the calibration distance in the **Scale** window.
NOTE: The distance should be similar to the separation of markers on the specimens. The calibration device offers three measuring distances: 10, 15 and 40 mm. Due to the 50 mm marker separation, the 40 mm distance is appropriate.
4. After calibration, change the marker type to **Pattern** in the **Targets** window.
NOTE: This enables the video extensometer to follow the markers indicated on the specimen.

9. Test performance
1. Prepare the test parameters in the TextXpert software.
NOTE: The prepared program must enable a test with a selected strain rate in the uniaxial stress case. It must be correlated with the video extensometer. The recorded parameters are the initial distance of the extensometer markers (L0), and result functions of time, grip displacements, current extensometer's markers distance, and force. The pre-load force of 50 N[17] is programmed and the L0 distance is adjusted after preloading.
2. Put the specimen along the machine main vertical axis and close the grips using the tubular spanner.
NOTE: The specimen must be located symmetrically to the grips in the vertical and horizontal directions.
3. Perform the tests with the selected constant strain rate until the specimens break (use 0.005, 0.001, and 0.0001 s^{-1} strain rates). For each strain rate, test at least two specimens in the warp direction and fill direction. Save the test results.
NOTE: The following data are necessary: the initial distance of the extensometer markers (L0), time functions of the extensometer's marker distance, and the force.

10. Repeat steps 1.5−1.9 every two weeks using the other sets of samples (six times, up to 12 weeks).
11. Repeat the entire procedure at 90 °C. The total number of specimens does not change. The ageing process lasts 6 weeks. Remove and test subsequent sets of specimens every week.

2. Data preparation

1. Knowing the cross section area of the samples, use graphing software (SigmaPlot[18] or similar) to recalculate the registered force and elongation increments according to elementary strength of material equations to the stress-strain relations. Plot a graph of obtained data, separately, for the warp and fill samples and for each of the strain rates.
2. Repeat for the 80 °C and 90 °C results.

3. Parameter identification of material models

1. Piecewise linear model for non-linear elastic modeling
NOTE: The application of the piecewise linear material model is possible when the stress-strain curve can be split into sections of linear (or approximately linear) shapes. Particular crossing points of the lines at neighboring sections correspond to applicability ranges of the related lines[19].
1. In the case of every curve obtained in step 2.1, find the strain ranges, detecting the linear or close to linear stress-strain relation.
2. Using the fit regression option in the graphing software and the least square method, identify the best-fit line in the chosen region.
NOTE: The tangent to this curve corresponds to the stiffness of the material in a particular range.
3. Denote the tangent as E_{ij} where the index **i** corresponds to the current direction of the material (W for the warp direction and F for the fill direction) and the index **j** is a consecutive number of the identified line.
4. Having parameters of all the lines, find the intersection points between the lines; denote them as $\varepsilon_{k/l}$, where **k** and **l** mark the crossing lines.
NOTE: These points ($\varepsilon_{k/l}$) constitute the strain ranges to apply the particular longitudinal stiffness values (E_{ij}) (**Figure 1**).

2. Bodner–Partom viscoplastic model
NOTE: The Bodner–Partom constitutive law is used to reflect the elasto-viscoplastic behavior of various materials[20,21]. The basics and mathematical formulation of the model is given in detail elsewhere[20,21,22,23,24,25]. The elementary equations are presented in **Table 1** only to model the uniaxial stress state. The Bodner–Partom model parameters are identified by means of the uniaxial tensile tests conducted with at least three different strain rates. The value of the strain rate must be constant at least in the inelastic part of the experiment. The complete Bodner–Partom model identification procedure modified for technical woven fabrics is widely presented[24,25].
1. Using the graphing software, identify Bodner–Partom model parameters following Klosowski et al.[24].

4. Arrhenius extrapolation

NOTE: The Arrhenius law is based on an empirical observation that ambient temperature increase results in acceleration of a number of chemical reactions that may speed up the ageing process as well. The complete mathematical representation of the Arrhenius chemical reaction concept can be found elsewhere[11,26]. The Arrhenius law in a simplified form is called "the 10 degree rule"[27]. According to this rule, a surrounding temperature increase of about 10 °C theoretically doubles the rate of the aging process. Hence, the reaction rate f is defined as follows[17]:

$$f=2^{\Delta T/10}, \qquad (1)$$

where $\Delta T = T - T_{ref}$ is the difference between the ageing temperature T and the service temperature T_{ref} of a material.

1. Assume the temperature T_{ref} according to the average value based on the results of the local meteorological station (here, T_{ref} = 8 °C[28]). Assume the thermal chamber temperature T to be used in the ageing test (here, 80 °C and 90 °C).
   NOTE: The temperature level should be registered for a longer time period, at least one year, and then calculated as the mean value of that period, bringing a time average of this period taken as T_{ref}.
2. Calculate the reaction rate constant **f** from equation 1 and then extrapolate the ageing time (expressed in weeks) to years (**Table 2**).
   NOTE: The extrapolation effects of different ageing time periods conducted within the current research are presented in **Table 3**. For instance, thermal ageing of a specimen in 4 weeks at 90 °C is equal to its ageing in 8 weeks at 80 °C and corresponds to a natural ageing of approximately 23 years.

5. Data representation

1. Present the obtained parameter values in the normalized form of **X/X⁰**, where **X** denotes a current value of the certain parameter and **X⁰** corresponds to the initial value of this parameter, with regard to a specimen aged 1 hour only.
   NOTE: The time of artificial thermal ageing is set up in hours.
2. Plot X/X⁰ values on the Y axis versus the ageing time plotted on the X axis to show the evolution of the parameters. Prepare plots for the warp and fill directions of the tested material separately.
3. Describe the parameter values plotted over time by linear functions (or different best-fit functions) using the least square method and report R^2 values.
4. To evaluate whether the Arrhenius simplified relation is correct for AF9032 fabric, redraw the results obtained for 90 °C with respect to the ageing time recalculated into "real" time according to the Arrhenius law.

Representative Results

Figure 2 juxtaposes the stress-strain curves for the warp and fill directions of AF9032 fabric obtained at different ageing times, in the 80 °C temperature level for a strain rate of 0.001 s^{-1}. The difference between the 1 h ageing period (reference test) and the rest of the ageing periods is clear. The ageing time does not seem to substantially affect the material response in the warp direction, as the stress–strain curves are highly repetitive, showing no important differences in the ultimate tensile strength (UTS). It stays contrary to the behavior observed for the fill direction, where the UTS is much lower in the case of artificially aged samples than in the unaged case. Moreover, the achieved stress–strain curves detect divergent trajectories when the strains exceed 0.06.

The results obtained at different temperature levels and the extrapolation of the results for a higher temperature level presented in one graph compress all the data concerning a particular parameter. If the curves representing evolution of the parameters in both temperatures over the ageing time fall into the same trajectory, it confirms that the obtained parameter values actually follow the Arrhenius equation. If the lines are parallel, it suggests that additional experiments are necessary to explain the observed phenomenon or that some correction coefficients should be introduced to the results at one temperature level to make results in both temperatures fall into one path.

Variation images of the PVC coating stiffness and fill ultimate strains over the ageing time are in **Figure 3** and **Figure 4**, respectively. The experimental results at two temperature levels of 80 °C and 90 °C are presented in **Figure 3a** and **Figure 4a**. It was proven before[24] that the first linear part of the experimental stress-strain curve of a simple tensile test (denoted here as E_{F0}) corresponds to the stiffness of technical fabric covering made of PVC. The results obtained at the temperature level of 90 °C extrapolated in hours to 12 weeks (2000 hours) and recalculated to "real" years according to the Arrhenius simplified relation are drawn in the same graph in order to compare the results (**Figure 3b** and **Figure 4b**).

The evolution of stiffness of the PVC coating over ageing time is almost linear at temperature levels of 80 °C and 90 °C with a constant increment in time, much greater in 90 °C than in 80 °C. This phenomenon suggests that PVC subjected to relatively high temperature undergoes changes resulting in the growth of its stiffness, as an effect of accelerated ageing. This behavior is possibly caused by physical ageing, specific for polymer materials, like technical fabrics. The ultimate tensile strains values (ε_{ult}) exhibit a decreasing trend over ageing time in the fill direction and temperature levels of 80 °C and 90 °C. For the warp direction, the UTS values show no significant variation over ageing time. On the other hand, the ultimate tensile strains (ε_{ult}) decrease in 80 °C and grow in 90 °C.

The same procedure has been used to address the Bodner–Partom model parameters. Here, the hardening parameter m_1 in the warp direction and the viscosity parameter n in the fill direction are presented in **Figure 5** and **Figure 6**, respectively.

The final research results are sets of linear functions, which represent certain material parameters or fabric properties over ageing time. Following this, all the basic mechanical properties (stiffness, yield limit, ultimate tensile stress and strain) and Bodner–Partom model parameters (n, D_0, D_1, R_0, R_1, m_1, m_2) were identified, put together at temperature levels of 80 °C and 90 °C and analyzed by means of the Arrhenius extrapolation methodology[29].

The approximation lines corresponding to the parameter trends throughout ageing time collapse to one line for UTS, ε_{ult}, m_1 in the case of fill direction. Other parameter approximation lines in ageing time exhibit parallel tendencies without collapse to one line.

In the case of warp direction, only the approximation lines of UTS, E_{W2} and m_1 collapse into one line, while other parameters show neither clear tendency nor parallel character of the curves. All the parameter values in ageing time for the fill direction express parallel trends or collapse to one line. Thus, the approach of the Arrhenius simplified equation, shown in the present article, has been proven for that direction only.
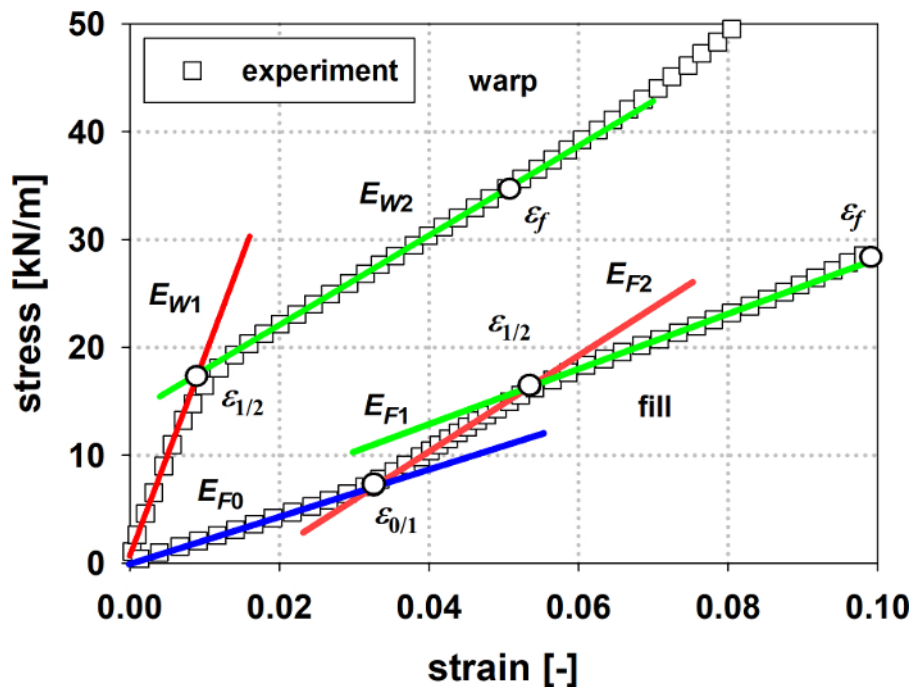
Figure 1: Schematic representation of the piecewise linear model for AF9032 fabric. Please click here to view a larger version of this figure.
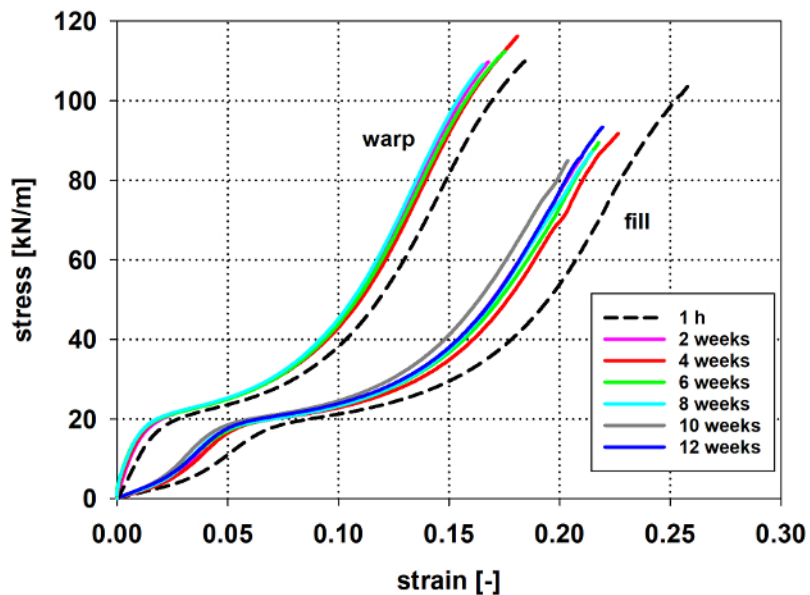

Figure 2: The impact in thermal ageing case at 80 °C on the stress–strain response in the warp and fill directions of AF9032 fabric, for the strain rate of 0.01 s^{-1}. Please click here to view a larger version of this figure.
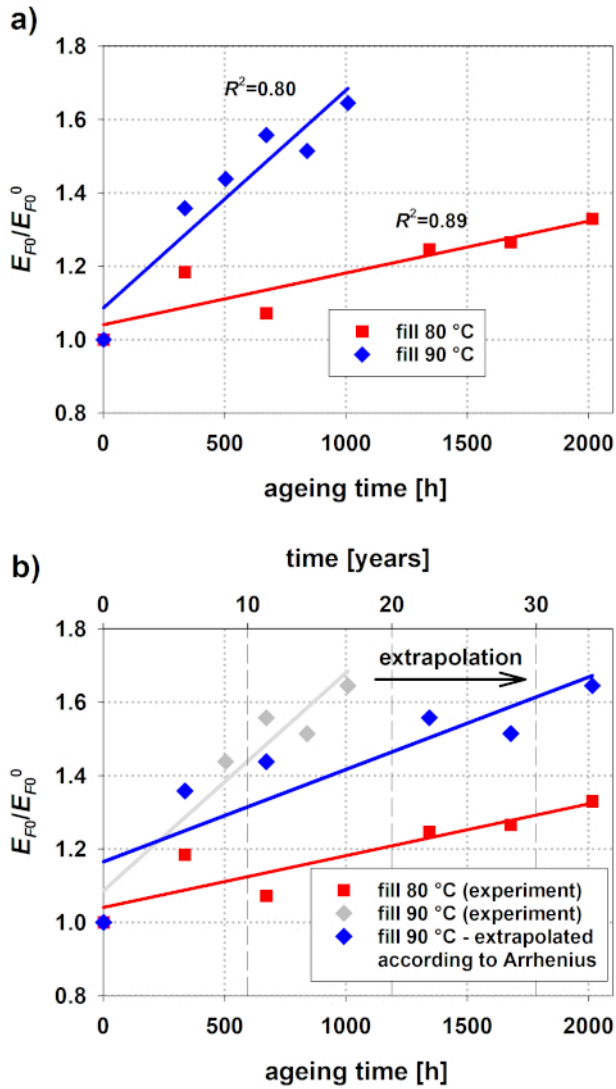
Figure 3: Stiffness of the PVC coating at different ageing times in hours (red and blue lines) (a); stiffness values obtained at 90 °C recalculated to time in years according to the Arrhenius simplified equation (blue lines) for the fill direction of AF9032 fabric (b). Please click here to view a larger version of this figure.
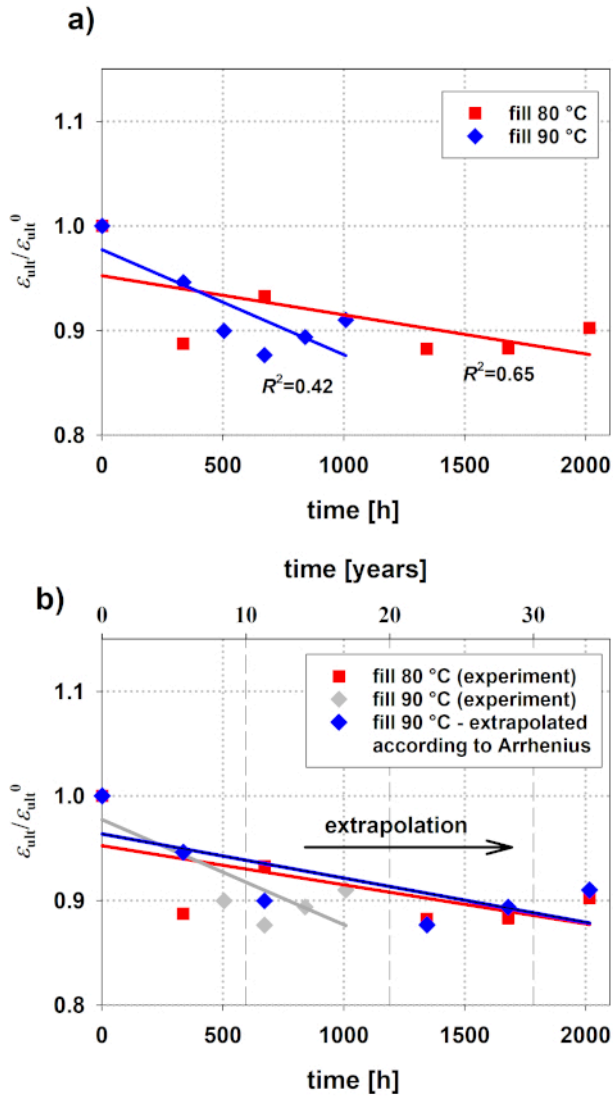
Figure 4: Ultimate strains of the PVC coating at different ageing times in (red and blue lines), experiments (a); ultimate strains values obtained at 90 °C recalculated to time in years according to the Arrhenius simplified equation (blue lines) in the fill direction of AF9032 (b). Please click here to view a larger version of this figure.
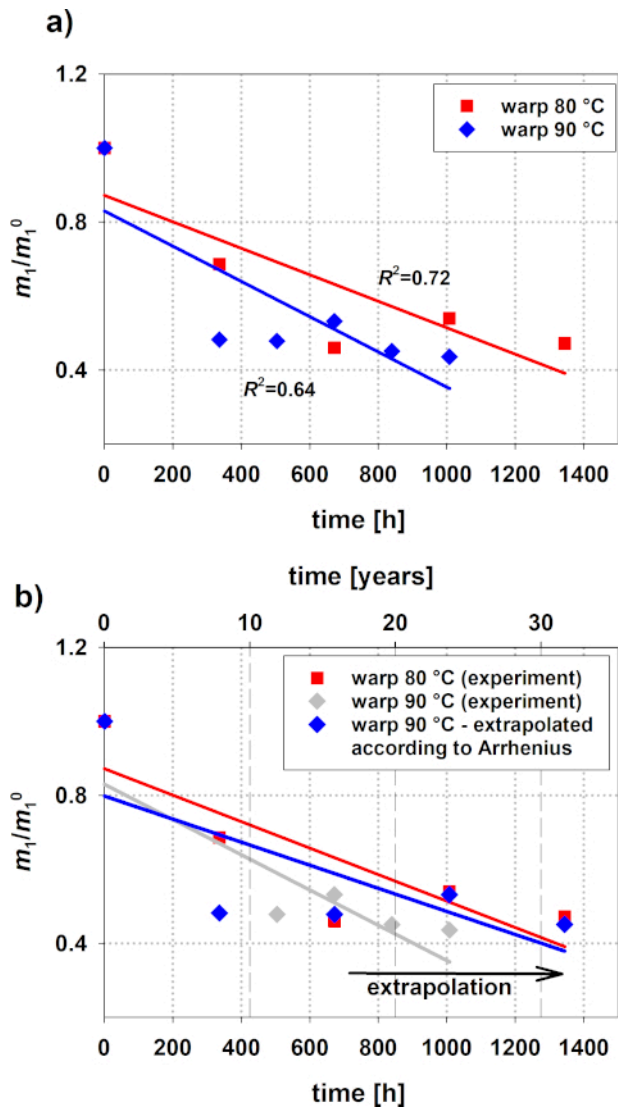
Figure 5: Bodner–Partom coefficient of isotropic hardening m_1 at different ageing times in hours (red and blue lines), experiments (a); coefficient of isotropic hardening m_1 values obtained at 90 °C recalculated to time in years according to the Arrhenius simplified equation (blue lines) in the warp direction of AF9032 (b). Please click here to view a larger version of this figure.
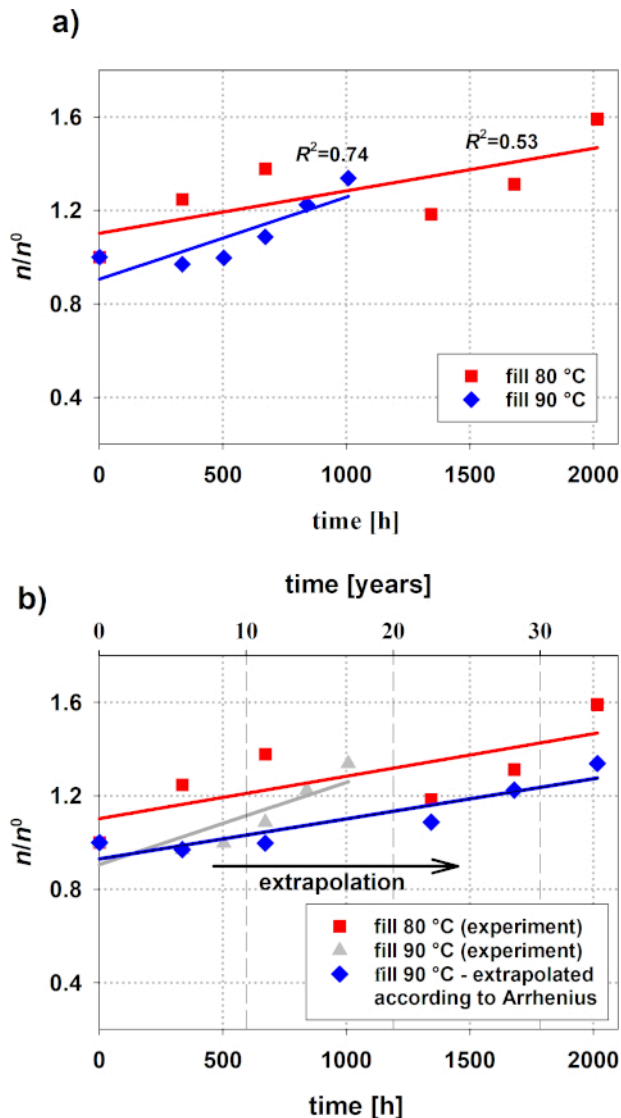
Figure 6: Bodner–Partom strain rate sensitivity parameter n at different ageing times in hours (red and blue lines) experiments (a); and strain rate sensitivity parameter n values obtained for 90 °C recalculated to time in years according to the Arrhenius simplified equation (blue lines) for the fill direction of the AF9032 (b). Please click here to view a larger version of this figure.

Inelastic strain rate	$\dot{E}^{I}=\dot{p}\,\mathrm{sig}(\sigma)$
Cumulated inelastic strain rate	$\dot{p}=\dfrac{2D_0}{\sqrt{3}}\exp\left[-\left(\dfrac{Z}{\lvert\sigma\rvert}\right)^{2n}\dfrac{n+1}{2n}\right]$
Additional equations	$Z=R+\sqrt{\tfrac{2}{3}}X\,\mathrm{sgn}(\sigma)$ $\dot{W}^{I}=\sigma\dot{E}^{I}$
Isotropic hardening	$\dot{R}=m_1\left(R_1-R\right)\dot{W}^{I},\quad R(t=0)=R_0$
Kinematic hardening	$\dot{X}=m_2\left(\sqrt{\tfrac{3}{2}}D_1\,\mathrm{sgn}(\sigma)-X\right)\dot{W}^{I}$
Material parameters	$n, D_0, D_1, R_0, R_1, m_1, m_2$

Table 1: Basis Bodner–Partom equations in uniaxial state.

Variable	T_{ref}	T	ΔT	f	Calculation example for 4 weeks of therml ageing
Formulation	-	-	$T - T_{ref}$	$2^{(\Delta T/10)}$	f*4/52
Unit	°C	°C	°C	[-]	[years]
Results	8	80	72	147	11.3
		90	82	294	22.6

Table 2: Example calculations of the Arrhenius simplified equation.

Laboratory ageing time [weeks]		1	2	3	4	5	6	7	8	9	10	11	12
Time according to Arrhenius [years]	80 °C	2.8	(5.7)	8.5	(11.3)	14.1	(17.0)	19.8	(22.6)	25.4	(28.3)	31.1	(33.9)
	90 °C	(5.7)	(11.3)	(17.0)	(22.6)	(28.3)	(33.9)	39.6	45.2	50.9	56.6	62.2	67.9
( ) marks the ageing tests performed in the present study and used to identify parameters.													

Table 3: Extrapolation of ageing time recalculated with the Arrhenius equation at temperature levels of 80 °C and 90 °C.

Discussion

This article incudes a detailed experimental protocol to simulate the laboratory accelerated experiments on polyester reinforced and PVC coated fabrics for civil engineering applications. The protocol describes the case of artificial thermal ageing only by the means of raising the ambient temperature. This is an obvious simplification of real weather conditions, as UV radiation and water influence play an additional role in material service ageing.

Generally, the conditions of accelerated ageing performed in the laboratory should be as close as possible to the true weather and service conditions of a tested material. For instance, materials used in aerospace or marine structures undergo hydrothermal ageing, when humidity and temperature primarily act upon the material durability[30,31]. Regarding the battery degradation level, two ageing factors are usually monitored: temperature and state of charge[9]. In electrical cable insulations, apart from temperature, different voltage and stress levels must be included, while performing accelerated laboratory ageing[14]. However, the thermal type of accelerated ageing is the most common one, thus it is easy to reflect it in the laboratory. The calibration of the obtained results with outdoor data of the service aged material creates a reliable tool to predict the future behavior of textile fabrics or other materials.

A drawback of the presented method is the number of samples tested. Because uniaxial tensile experiments with three different constant rates are conducted, two samples were tested in each material direction for each strain rate case. As the analysis has to cover both warp and fill directions of the fabric, tested at two temperature levels, with at least 5 ageing time intervals, a large number of samples is required. Fortunately, the results are very repetitive, displaying very similar tendencies; therefore, the obtained results are considered reliable even if two samples are tested in the same conditions only.

The procedure for conducting the uniaxial tensile tests with constant strain rates and with the video extensometer data registration is presented thoroughly. The European national standard[1] does not require the use of an extensometer for testing technical fabrics. Therefore, the proposed protocol is more precise than the standard requirements; thus, the obtained data are more accurate.

The proposed protocol makes it possible to determine material parameters for fabrics in the future; therefore, it is a suitable tool in design. The method has been successfully validated during the research of the hanging roof of the Forest Opera in Sopot. The samples of the polyester reinforced, and PVC coated fabrics were collected from the roof after 20 years of operation. Samples of unaged material were also obtained from the same manufacturer. Both types of samples proceeded through the same laboratory experiments and parameter identification routines. Results were represented by the parameters of the piecewise linear and Bodner–Partom models. The trends observed in mechanical behavior of material from the Forest Opera resemble trends found in the case of thermal ageing. Thus, the results presented here have been confirmed by the tests of a fabric after 20 years of service[28]. Nevertheless, for other kinds of technical fabrics, some modifications of the proposed method may be required, thus the experimental protocol should be properly adjusted.

Disclosures

The authors have nothing to disclose.

Acknowledgments

References

1. Ambroziak, A. Mechanical properties of Precontraint 1202S coated fabric under biaxial tensile test with different load ratios. *Construction and Building Materials.* **80**, 210-224 (2015).
2. Żerdzicki, K., Kłosowski, P., Woźnica, K. Analysis of the cyclic load-unload-reload tests of VALMEX aged fabric. In *Shell Structures: Theory and Applications.* Edited by Pietraszkiewicz, W., Witkowski, W., 477-480, CRC Press. Boca Raton, FL (2017).
3. Cash, C. G., Bailey, D. M. *Predictive service life tests for roofing membranes: Phase 2. Durability of Building Materials and Components.* Taylor, Francis. London (2014).
4. Yin, W. et al. Aging behavior and lifetime prediction of PMMA under tensile stress and liquid scintillator conditions. *Advanced Industrial and Engineering Polymer Research.* **2** (2), 82-87 (2019).
5. Swedish Standards Insitute. Buildings And Constructed Assets - Service Life Planning - Part 7: Performance Evaluation For Feedback Of Service Life Data From Practice. *International Organization of Standardization.* 15686-7, 2006 (2017).
6. Šaršounová, Z. The Inconveniences Related to Accelerated Thermal Ageing of Cables. *Transportation Research Procedia.* **40**, 90-95 (2019).
7. Gong, Y. et al. Comparative study on different methods for determination of activation energies of nuclear cable materials. *Polymer Testing.* **70** (June), 81-91 (2018).
8. Vega, A., Yarahmadi, N., Jakubowicz, I. Optimal conditions for accelerated thermal ageing of district heating pipes. *Energy Procedia.* **149**, 79-83 (2018).
9. Redondo-Iglesias, E., Venet, P., Pelissier, S. Eyring acceleration model for predicting calendar ageing of lithium-ion batteries. *Journal of Energy Storage.* **13**, 176-183 (2017).
10. Panjan, P., Virtanen, V., Sesay, A. M. Determination of stability characteristics for electrochemical biosensors via thermally accelerated ageing. *Talanta.* **170** (April), 331-336 (2017).
11. Martin, R. *Ageing of Composites.* Woodhead Publishing (2008).
12. Mouzakis, D. E., Zoga, H., Galiotis, C. Accelerated environmental ageing study of polyester/glass fiber reinforced composites (GFRPCs). *Composites Part B: Engineering.* **39** (3), 467-475 (2008).
13. Rosato, D., Rosato, M. *Plastic product material and process selection handbook.* Elsevier: Kidlington, Oxford (2004).
14. Brebu, M. et al. Study of the natural ageing of PVC insulation for electrical cables. *Polymer Degradation and Stability.* **67** (2), 209-221 (2000).
15. Martienssen, W., Warlimont, H. *Handbook of Condensed Matter and Materials Data.* Springer Berlin: Berlin (2005).
16. Berard, M.T., Daniels, C.A., Summers, J.W., Wilkes, C.E. *PVC Handbook.* Munchen: Hanser (2005).
17. *Rubber – or plastics-coated fabrics – Determination of tensile strength and elongation at break.* Beauth Publishing. SN EN ISO 1421 (2017).
18. Systat Software, Inc. *SigmaPlot 12.0 User's Guide.* (2015).
19. Ambroziak, A., Kłosowski, P. Mechanical testing of technical woven fabrics. *Journal of Reinforced and Plastic Composites.* **32** (10), 726-739 (2013).
20. Bodner, S.R., Partom, Y. Constitutive equations for elastic–viscoplastic strain-hardening materials. *Journal of Applied Mechanics.* **42**, 385-389 (1985).
21. Andersson, H. An implicit formulation of the Bodner–Partom constitutive equations. *Computers and Structures.* **81** (13), 1405-1414 (2003).
22. Kłosowski, P., Zagubień, A., Woznica, K. Investigation on rheological properties of technical fabric "Panama." *Archive of Applied Mechanics.* **73** (9–10), 661-681 (2004).
23. Zaïri, F., Naït-Abdelaziz, M., Woznica, K., Gloaguen, J. M. Constitutive equations for the viscoplastic-damage behaviour of a rubber-modified polymer. *European Journal of Mechanics, A/Solids.* **24** (1), 169-182 (2005).
24. Klosowski, P., Zerdzicki, K., Woznica, K. Identification of Bodner–Partom model parameters for technical fabrics. *Computers and Structures.* **187** (2017).
25. Zerdzicki, K. Durability evaluation of textile hanging roofs materials. *Ph.D Thesis Gdansk University of Technology.* (2015).
26. Bystritskaya, E. V., Pomerantsev, A. L., Rodionova, O. Y. Prediction of the aging of polymer materials. *Chemometrics and Intelligent Laboratory Systems.* **47** (2), 175-178 (1999).
27. Hukins, D. W. L., Mahomed, A., Kukureka, S. N. Accelerated aging for testing polymeric biomaterials and medical devices. *Medical Engineering and Physics.* **30** (10), 1270-1274 (2008).
28. Zerdzicki, K., Klosowski, P., Woznica, K. Influence of service ageing on polyester-reinforced polyvinyl chloride-coated fabrics reported through mathematical material models. *Textile Research Journal.* **89** (8), 1472-1487 (2019).
29. Klosowski, P., Zerdzicki, K., Woznica, K. Influence of artificial thermal ageing on polyester-reinforced and polyvinyl chloride coated AF9032 technical fabric. *Textile Research Journal.* **89** (21–22), 4632-4646 (2019).
30. Firdosh, S. et al. Durability of GFRP nanocomposites subjected to hygrothermal ageing. *Composites Part B: Engineering.* **69**, 443-451 (2015).
31. Le Saux, V., Le Gac, P. Y., Marco, Y., Calloch, S. Limits in the validity of Arrhenius predictions for field ageing of a silica filled polychloroprene in a marine environment. *Polymer Degradation and Stability.* **99** (1), 254-261 (2014).